



ISSN: 1813-162X (Print) ; 2312-7589 (Online)

Tikrit Journal of Engineering Sciences

available online at: <http://www.tj-es.com>

**TJES**  
Tikrit Journal of  
Engineering Sciences

Mahmood AM, Mohammad KI. Finite Element Analysis for RC Deep Beams under an Eccentric Load. *Tikrit Journal of Engineering Sciences* 2019; 26(1): 41-50.

Bashar A. Mahmood\*

Khalaf I. Mohammad

Department of Civil Engineering  
College of Engineering  
University of Mosul  
Mosul  
Iraq

## Finite Element Analysis for RC Deep Beams under an Eccentric Load

A B S T R A C T

This study investigates the effect of the load eccentricity on the deep beams, in terms of failure load and failure mode, using ANSYS nonlinear finite element program. Three RC deep beams with shear span to depth ratios, varying from 0.91 to 1.67 are modeled. A comparison between the experimental and numerical results, under central load, showed approximately full matching between them. This had been done in order to ensure that the model was represented properly. The used model for investigating the behavior of the RC deep beams under an eccentric load with various heights of beams showed that under eccentric load there was a significant reduction in the failure load. Increasing the beams height cause of an increase (gradually) of the failure load with the incremental increases of the height, also there was a clear reduction in the failure load due to eccentricity. For the load eccentricity value 50 mm all the beams of different heights possess the same failure load and all of them failed due to concrete crushing at the beam compression face.

**Keywords:**

Deep Beams  
Eccentricity  
Finite Element  
Reinforced Concrete

### ARTICLE INFO

**Article history:**

Received 05 November 2018  
Accepted 22 January 2019  
Available online 01 March 2019

© 2019 TJES, College of Engineering, Tikrit University

DOI: <http://dx.doi.org/10.25130/tjes.26.1.06>

## تحليل العتبات الخرسانية العميقة تحت تأثير الاحمال غير المركزية باستخدام طريقة العناصر المحددة

بشار عبد العظيم محمود، خلف ابراهيم محمد

قسم الهندسة المدنية، كلية الهندسة، جامعة الموصل

الخلاصة

يهدف هذا البحث الى دراسة تأثير الاحمال غير المركزية على العتبات الخرسانية المسلحة العميقة من ناحية قيمة حمل الفشل ونمط الفشل باستخدام برنامج ANSYS بطريقة العناصر المحددة اللاخطية. تمت نمذجة ثلاثة عتبات خرسانية مسلحة بنسب فضاءات قص العمق متغيرة من 0.91 الى 1.67. المقارنة بين نتائج الفحوصات المختبرية و التحليلات العددية تحت تأثير الاحمال المركزية اظهرت تطابقا شبه تام بينهما حيث ان هذا يؤكد ان النموذج العددي قد مثل الواقع الفعلي بصورة صحيحة. تم استخدام النموذج للتحقق من سلوك العتبات الخرسانية العميقة تحت الاحمال اللامركزية لإرتفاعات مختلفة للعتبات، حيث لوحظ ان انخفاضاً ملحوظاً في قيمة حمل الفشل تحت تأثير الاحمال اللامركزية. لوحظ انه بزيادة ارتفاع العتبات قد زاد حمل الفشل تدريجياً مع كل زيادة في الارتفاع وكذلك يلاحظ ان هنالك انخفاض واضح في حمل الفشل بسبب لامركزية الاحمال، ولكن عندما يصل انحراف الحمل المسلط على العتبات إلى 50 ملم ، فإن جميع العتبات بغض النظر عن ارتفاعها انها تمتلك نفس قيمة حمل الفشل حيث ان جميعها فشلت بسبب انسحاق الخرسانة في الوجه المعرض للانضغاط.

\* Corresponding author: E-mail : [Bashargxabd@gmail.com](mailto:Bashargxabd@gmail.com)

## 1. INTRODUCTION

RC deep beam are widely used elements in buildings, bridges, infrastructures, high-rise buildings as load-distributing structural parts of transfer girders, in multistory buildings to provide column offsets, wall footing, foundation pile caps, walls of rectangular tanks and bins, floor diaphragms, and shear walls [1]. The behavior of the reinforced concrete deep beams are influenced by many factors, such as clear span/ depth ratio, shear span / depth ratio, type of loading, position of the load, amount and type of web reinforcement, concrete strength [2]. It was characterized by a relatively large depth compared to the span of the beams. by (American Institute of Concrete) [3]. Deep beams, are those beams that possess clear span does not exceed more than four times the overall member depth  $h$ , or concentrated load exist within a distance  $2h$  from the support face. Till now, there is no specific definition for deep beams.

A series of studies on deep beams have been carried out. Tan [4] studied the influence of the effective span-depth ratio with different web reinforcements, their effect on the behavior of the high strength concrete deep beams. Siao [5] investigated the shear strengths of short reinforced concrete walls, corbel, and deep beams. Most of these studies were based on the analysis of an experimental results under a centric load. Patil et al. [6] worked on analyzed a deep beams subjected to two loading points with three different L/D ratios (1.5, 1.6, 1.71) using a Non-linear finite element method (ANSYS 9.0 software). This had been done in order to investigate the stress and strain distribution pattern at mid-section of the beam. It was found that as the span/depth ratio is smaller, as more pronounced deviation of strain pattern at mid-section of the beam. Flexural stress and strain variation graphs are indicated that when L/D ratio is less than or equal to 2.0 then the results are reasonably accurate. From the flexural strain and stress graphs it was observed that as L/D ratio of the beam decreases the neutral axis would be shifted towards the soffit region in the beam.

Plasencia et al. [7] studied the behavior of a reinforced concrete deep beams by numerical simulation. His results were calibrated and validated by a comparison with a previous experimental results. In modeling, it was assumed a bilinear model with Von Mises failure criteria for steel and Concrete Plasticity Damage for the concrete, achieving an appropriate matching between the numerical and experimental reference. This feature that allowed the parametric study of the influence of the geometric factors and reinforcement. The results showed that, increasing the amount of main reinforcement in the beams, then shear capacity increases, reaching a limit where the increasing amount come to be not significant, because the failure is determined by the behavior of the strut. Increasing the amount of the vertical reinforcement would increase the shear capacity. And increasing of the amount of the horizontal web reinforcement has a moderate effect on the shear capacity. Salamy et al. [8] studied the behavior of RC deep beams by means of finite element analysis

along with an experiments. The beams have a (shear span / depth) ratio between 0.5 and 1.5 and effective depth from 400 mm to 1400 mm. Lateral reinforcement ratio varies as follow, 0.0%, 0.4% and 0.8% in the shear span. The fracture type analysis was employed to simulate RC members through smeared rotating crack approach. The objective of this study is to investigate the capabilities of the finite element simulation for further study on deep beam behavior instead of conducting an expensive time and experimental works. The results showed the reliability degree of the analysis in predicting the deep beams behavior in terms of failure load, failure mode as well as crack propagation. Lafta and Kun YE [9] used the ANSYS finite element program to study the behavior of indirectly loaded deep reinforced concrete (RC) of T-beams, A total number of 21 deep RC T-beams were divided into three groups according to their (shear span / effective depth) ratio. Beams without web reinforcement were tested using indirect point loading that applied via central intersecting members till shear failure, Ultimate loads, deflection responses, and crack patterns are recorded as well. the predicted ultimate failure load value was close to that obtained by the experimental test, the mid-span deflections of the indirectly loaded, flanged deep beams were less than the permissible deflections that specified by ACI Building Code (318-11) and the crack pattern showed that the webs of all beams were functioned as a simple struts between loads and supports. Sabale [10] used the ANSYS program to study the behavior of a deep beam of various (span / depth ratio) under two loading points of 50kN. The objectives of this study are to observe deflection, cracking of deep beams that subjected to two loading points of 50KN. To study the non- linear finite element analysis of the deep beam using ANSYS, that having different (L/D) ratios (1.5, 1.6, 1.71) and to study stress distribution of deep beam. Deflection of beams increases as (span / depth) ratio decreases and as (span / depth) ratio continue decreasing, then the failure load continue decreasing. Kumar and Ramadass [11] worked on an attempt to predict the shear strength for concrete deep beams at ultimate state, using ANSYS software; two test beams had been accounted to predict their shear strength at ultimate state. The accuracy of the predicted values of shear strength that based on ANSYS 12.1 software for the two test beams were compared with their corresponding experimental results. For beam specimen S0.3/0.5 the shear strength is found to be 9.93% higher in magnitude, compared with the corresponding experimental results. For beam specimen S0.3/1.0, the shear strength was found to be 9.65% higher in magnitude compared with the corresponding experimental results.

There are few theoretical researches in studying the behavior of deep concrete under eccentric loads.

Experimentally, in the test procedure the loads always applied on the central axis of the beam but practically (in buildings) it is difficult to insure to do that, whether the loads that coming from columns or bridges. There are a few experimental researches in this area. Chemrouk [12] worked on one and two span slender deep beams under centric and eccentric load. The main variables were the (height / thickness) ratio and the

quantity and arrangement of web steel. The results showed that the failure load depends mainly on the slenderness ratio (h/b) under the centric and eccentric load. Where failure mode transformed from shear to bulking failure. Belhacene et. al [13] worked on a high strength eccentrically loaded slender reinforced concrete deep beams with a vertical edge restraints, buckling tests were carried out on 6 reinforced concrete deep beams having (height/thickness) ratios in the range 25 to 67. Observations were made on the ultimate loads and failure modes, the variables studies were included, (height / thickness) and (eccentricity / thickness) ratios. They concluded that when the vertical edges of the slender deep beam are restrained, then an unintentional eccentricity up to 0,2 times the beam thickness (b) will not change the failure mode which usually shear when loads are centrally applied and the failure mode is strongly dependent of the load (eccentricity/thickness) ratio (e/b). An increase in the (e/b) ratio would significantly increase the likelihood of the failure mode that changing from shear to buckling. Kim etal [14] worked an empirical studies on a reinforced concrete deep beam behaviors under mutual bending and the axial loads in order to inspect the effect of the axial loads on structural performance of the reinforced concrete deep beams; samples of various (shear span/depth) ratios were exposed to an axial loads of 235 kN or 470 kN. They observed that the structural behaviors such as, load deflection response, strain in concrete and steel bar. The results showed that the deep beam with shear (span/depth) ratio of (0.5) load failure of the deep beam decreases as the applied axial loads increasing. For deep beams with shear (span/depth) ratio of (1) and (1.5) showed that the applied axial loads make a delay the beam failure. When the shear (span/depth) ratio decreased, the failure mode of the deep beam transformed from shear failure to a concrete crushing compressive stress at the top corners of the reinforced concrete deep beams as shear (span/depth) ratio reduces. It is necessary to note that the deep beam with relatively small (span/depth) ratio under an axial load shows premature failure due to concrete crushing.

CIRIA guide [15] is the only document which gives recommendations on the strength of the slender deep beams except the new Euro-code2 [16] gives a very brief recommendations in this area and another technical document based on an elastic analysis but still in use is that published by the PCA [17].

The objective of this paper is to develop a numerical models for RC deep beams and to observe their behaviors under an eccentric load using ANSYS.

## 2. FINITE ELEMNET MODELING

Concrete is a quasi-brittle material that exhibits different behavior in compression and tension. ANSYS provides an element known as a SOLID65 that can be used in concrete modeling. This solid can crack in tension and crush in compression. The element consists

of 8 nodes having three degrees of freedom at each node [18].

The bearing plates and supports were modeled using a SOLID45 element. This is similar to the SOLID65 element with eight nodes and three degrees of freedom. This element was specifically used to distribute the load to prevent stress concentrations which would effect the convergence [18].

Steel reinforcement was modeled using LINK8. The element is a uniaxial tension-compression element with three degrees of freedom at each node, [18].

SOLID65 element requires linear isotropic and multi-linear isotropic material properties to proper concrete model. The multi-linear isotropic material uses the Von Mises failure criterion along with the Willam and Warnke [19] model to define the failure of the concrete. The compressive uniaxial stress-strain relationship for the concrete model was obtained using the following equations to compute the multi-linear isotropic stress-strain [20]. The modulus of elasticity was based on Eq. (3) [ACI-ASCE Committee 445-1998]. The elastic modulus of concrete was calculated for each beam using the slope of the tangent to the stress-strain curve through the zero stress and strain point.

$$f = \frac{Ec \epsilon}{1 + \left(\frac{\epsilon}{\epsilon_0}\right)^2} \dots \dots \dots (1)$$

$$\epsilon_0 = \frac{2fc'}{Ec} \dots \dots \dots (2)$$

$$Ec = 4730 \sqrt{fc'} \dots \dots \dots (3)$$

Where

$f$  = Stress at any strain ( $\epsilon$ ), MPa

$\epsilon$  = Strain at stress ( $f$ )

$\epsilon_0$  = Strain at the ultimate compressive strength,  $f_c'$

$Ec$  = Modulus of elasticity, MPa

The simplified stress-strain curve for each beam is constructed from several points that connected by a straight lines. Poisson's ratio equal to 0.2 is used. Shear retention factor, was assumed to be 0.7 for the closed cracks and 0.3 for the opened cracks. Tension stiffening factor (TC) was assumed to be 0.6.

SOLID 45 was used to simulate the plate with an elastic modulus equal to 200 GPa and Poisson's ratio equal to 0.3.

The steel reinforcement was assumed to be an elastic-perfect plastic material and identical in tension and compression. Elastic modulus and yield stress for the steel reinforcement were used in tests which was considered in the finite element modeling of the reinforcement. Poisson's ratio of 0.3 is adopted.

RC deep beams that tested by Ismail [21] have been chosen to be simulated by ANSYS. The author carried out tests on three RC deep beams (G1, G2 and G3) with (a/d) ratios equal to (1.67, 1.29, 0.91) respectively. These Beams were tested experimentally with zero eccentricity loads. Tables 1 and 2 show the properties of the G series.

Typical details of the tested beam G2 is shown in Fig. (1).

Typical finite element mesh, loading, and support simulation are shown in Fig. (2). Mesh size was selected as 50 mm in X-Y directions, and in Z direction ranging from 15-20 mm to simulate the load eccentricity. Fig. (3) shows the simulation of load eccentricity and supporting. Fully bond between the bar element nodes and concrete element nodes was assumed. The benefit of symmetry in modeling was ignored in order to simulate the actual boundary conditions of the experimental work.

**Table 1**

Properties of Tested Beams [21]

specimens	G1	G2	G3
a/d	1.67	1.29	0.91
$f_c$ (MPa)	30.9	30.5	31.3
$f_t$ (MPa)	3.4	3.1	3.3
$E_c$ (MPa) Eq.3	26293	26122	26462
Poisson ratio	0.3	0.3	0.3
V.Shear Reinf ratio %	0.56	0.59	0.67
H.Shear Reinf ratio%	0.215	0.215	0.215

**Table 2**

Steel Properties [21]

Bar Diameter (mm)	6	8	12	16
Area $mm^2$	28	50	113	199
Young's Modulus E (GPa)	200	200	200	200
Yield Stress $F_y$ (MPa)	577	448	404	364
Poisson ratio	0.2	0.2	0.2	0.2

### 3. NONLINEAR SOLUTION

In a nonlinear analysis of the total applied load using a finite element model which was divided into a series of load increments, that's called load steps. At the completion of each incremental solution, the stiffness matrix of the model is adjusted to reflect the nonlinear changes in the structural stiffness before proceeding to the next load increment. Newton–Raphson equilibrium iterations for updating the model stiffness were used in the nonlinear solutions. Prior to each solution, the Newton–Raphson approach assesses the out-of-balance load vector, which is the difference between their storing forces (the loads corresponding to the element stresses) and the applied loads. Subsequently, the program carries out a linear solution using the out-of-balance loads and checks for convergence. If the convergence criteria are not satisfied, the out-of-balance load vector is re-evaluated, the stiffness matrix is updated, and a new

solution is carried out. This iterative procedure continues until the results converge [18].

In this study, displacement convergence criteria were adopted and the maximum displacement convergence tolerance was set to 5%.

## 4. RESULTS AND DISCUSSIONS

A comparison between the experimental and numerical analysis was performed. This comparison included load-deflection response and failure load. The parametric study included load eccentricity and height of deep beam.

### 4.1. Load- Deflection Response

Fig. (4) show the points location of the measured deflections. Fig.(5) show a typical load-deflection response of beam G2 and represent a comparison between the experimental and the numerical load-deflection curves for the deflection at mid length of beams (G2) under a centric load and the beam behavior under the eccentric load. At central load with  $e = 0$  mm, the load-deflection response that predict from FE using ANSYS are approximately fully match with experimental load-deflection response.

Table 3 shows the percent of dropping in failure load due to eccentricity ( $e$ ) on the beams. At  $e=15$  mm for beams G1 and G2 the failure load owns the dropping percent 19.6% and 21.2% respectively but for beam G3 has dropping in failure load equal to 33.6% that's mean with shear span decreases under  $e = 15$  mm the dropping percent in the failure load increased, and the failure of the three beams are strut crush failure at the same ( $e$ ). When  $e = 30$  mm the dropping in the failure load (27.4%, 32.2% and 47.8%) for (G1, G2 and G3) respectively and from Fig. 9 even though they have different reduction ratios and they have different shear span but approximately they have the same failure load. For  $e = 50$  mm and from Fig.9 these beams under this value of eccentricity also they have the same failure load with different shear spans. Figs. (6, 7 and 8) show the load-lateral deflection response of beam G2 under the eccentric load, When ( $e$ ) increases, the ruling control for failure convert from strut failure to a concrete crush at the beam compression face.

### 4.2. The effect of the beam height on its behavior

Beams (G1, G2, and G3) were studied where the height was increased gradually from 500 mm to 800 mm with an incremental of 100 mm. Beams G1, G2, G3 with different heights were analyzed under an eccentric load at eccentricity of (0, 15, 30, and 50) mm, using finite element method only. Beam G2 was chosen as a typical model for numerical results. The increase in the beam height leads to an increase in the failure load at zero eccentricity. But with applying eccentric load on the beams a reduction in the failure loads is recorded with increase load eccentricity.

Figs. (10, 12, 14 and 17) showed a typical load deflection responses for beams G2 under centric and

eccentric load, Figure 16 showed the load-deflection comparison between the beam heights, G2. Dropping in failure load due to the eccentric load is shown in Figs. (11, 13, 15, and 18). Table 3 and Fig. (19) show the change and the dropping percentage in the failure load for each change in the height and eccentricity.

At eccentricity value of 15 mm, failure mode was strut crushing. The combined strut crushing and crushing of concrete in compressive face was indicated at  $e = 30$  mm. But when the eccentricity of the load on the beams reached 50 mm, then all beams with different heights

possessed the same failure load and all of them are failed due to concrete crush at the beam compressive face.

With increasing of eccentricity, the effect of the shear span becomes negligible for all heights of beams. (Figs. 11, 13, 15, and 18). Fig (20) shows the principal stresses (S1) in concrete of beam G2 at the compressed front face and at the tensile rear face before cracks. The stresses in the steel reinforcement at failure of beam G2 are shown in Fig.21, which not reached the yield stress in rear face due to concrete crush at the front face of the beam.

**Table 3**

Change in loads failure at eccentricity 0,15,30,50 mm and percentage dropping in failure load

<b>e = 0 mm for G1</b>			<b>e = 15 mm for G1</b>			<b>e = 30 mm for G1</b>			<b>e = 50 mm for G1</b>		
<b>h/b</b>	<b>Failure load (kN)</b>	<b>Drop in failure load %</b>	<b>h/b</b>	<b>Failure load (kN)</b>	<b>Drop in failure load %</b>	<b>h/b</b>	<b>Failure load (kN)</b>	<b>Drop in failure load %</b>	<b>h/b</b>	<b>Failure load (kN)</b>	<b>Drop in failure load %</b>
4	304.46	0	4	244.8	19.59	4	221	27.4	4	158.4	47.97
5	404.25	0	5	291.9	27.7	5	262.5	35	5	172.2	57.4
6	454.65	0	6	327.6	27.9	6	297.15	34.6	6	163.2	64.08
7	528.15	0	7	414.75	21.7	7	320.25	39.3	7	168	68.1
8	565.4	0	8	416.73	26.2	8	337.56	40.2	8	163.56	70
<b>e = 0 mm for G2</b>			<b>e = 15 mm for G2</b>			<b>e = 30 mm for G2</b>			<b>e = 50 mm for G2</b>		
<b>h/b</b>	<b>Failure load (kN)</b>	<b>Drop in failure load %</b>	<b>h/b</b>	<b>Failure load (kN)</b>	<b>Drop in failure load %</b>	<b>h/b</b>	<b>Failure load (kN)</b>	<b>Drop in failure load %</b>	<b>h/b</b>	<b>Failure load (kN)</b>	<b>Drop in failure load %</b>
4	363.8	0	4	286.4	21.2	4	246.4	32.2	4	175	51.8
5	444.5	0	5	330.6	25.6	5	291.45	34.4	5	180	59.5
6	572.25	0	6	405	29.13	6	320.25	44	6	176.4	69.17
7	572.2	0	7	383.25	33	7	336	41.2	7	176.4	69.1
8	620	0	8	416.32	32.9	8	343.2	44.6	8	186.2	69.8
<b>e = 0 mm for G3</b>			<b>e = 15 mm for G3</b>			<b>e = 30 mm for G3</b>			<b>e = 50 mm for G3</b>		
<b>h/b</b>	<b>Failure load (kN)</b>	<b>Drop in failure load %</b>	<b>h/b</b>	<b>Failure load (kN)</b>	<b>Drop in failure load %</b>	<b>h/b</b>	<b>Failure load (kN)</b>	<b>Drop in failure load %</b>	<b>h/b</b>	<b>Failure load (kN)</b>	<b>Drop in failure load %</b>
4	507.52	0	4	318	37.33	4	249.9	50.57	4	196.5	61.27
5	513.27	0	5	354.5	30.9	5	303.18	40.9	5	171.15	66.6
6	607	0	6	391.65	21.8	6	313	37.3	6	172.8	65.6
7	599.3	0	7	420.75	29.8	7	330	44.9	7	172.5	71.2
8	667	0	8	404.18	39.4	8	342.15	48.7	8	166.5	74.9

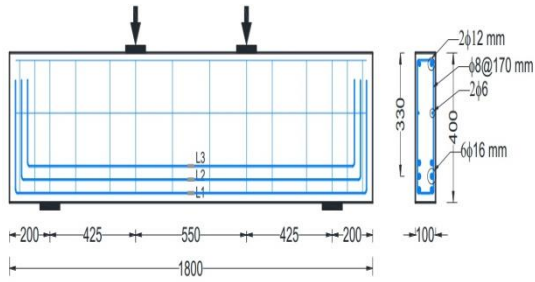


**Fig. 1.** Details of the tested beam (G2) all dimension in (mm) [16]

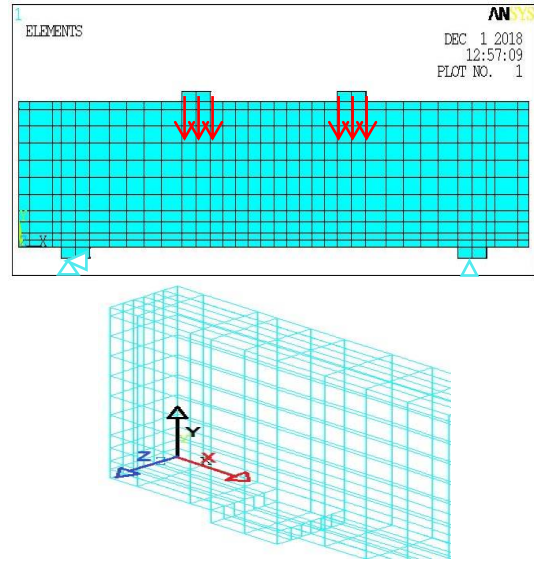


**Fig. 2.** Finite element mesh, loading, support simulation, and axes directions

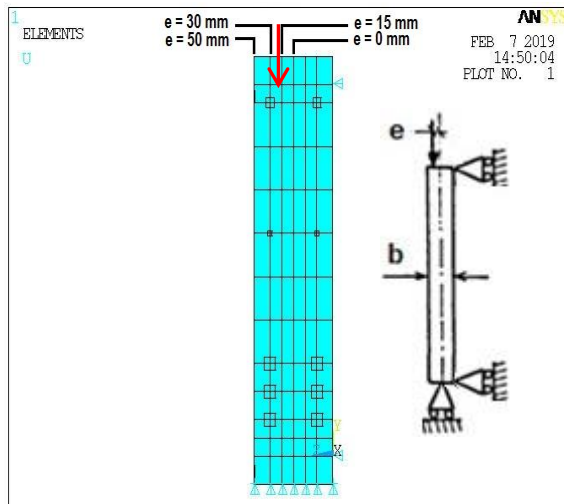


**Fig.3.** 3D and side view of the G2 beam under eccentric load and support condition

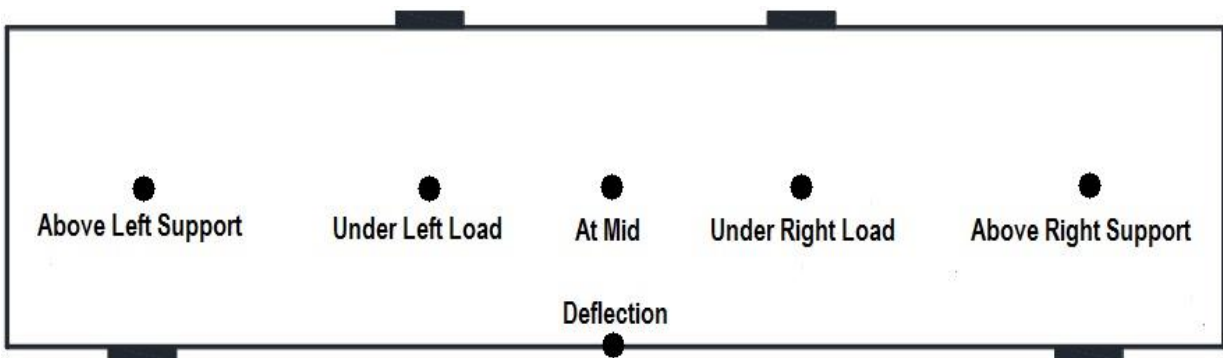
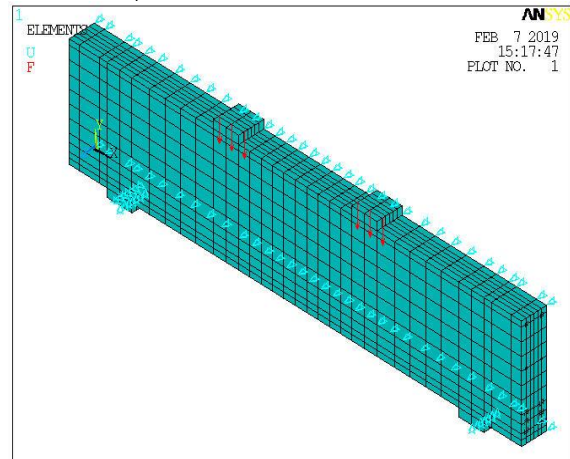


**Fig. 4.** Points at which the deflections were measured (G2)

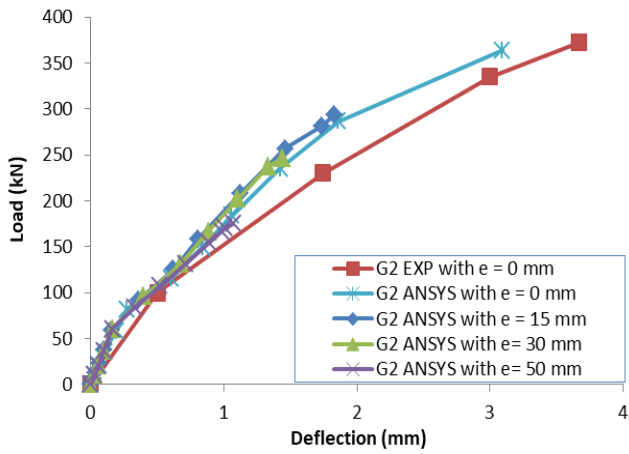


**Fig.5.** Eccentric Load-Deflection response of the Beam G2

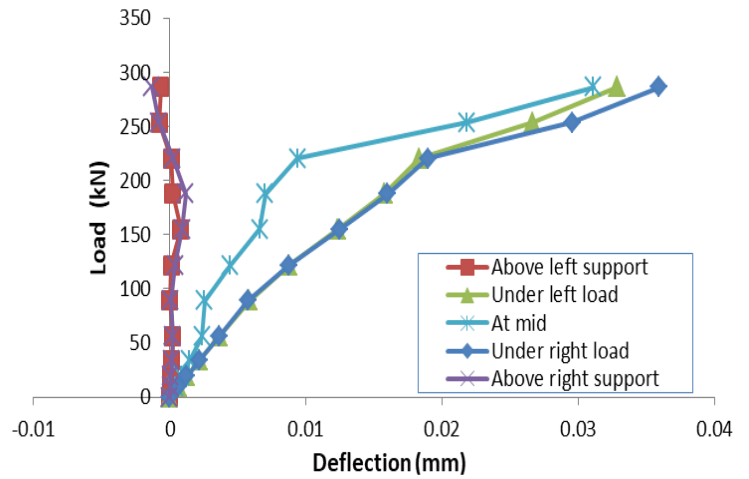


**Fig.6.** Typical Load-Lateral deflection curve of the Beam G2 e = 15 mm

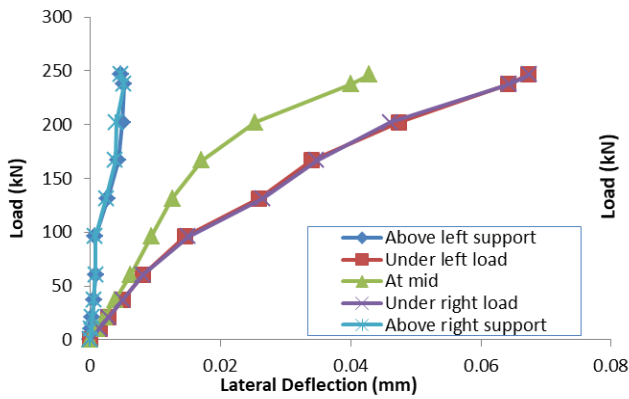


**Fig.7.** Typical Load- lateral deflection curve of the Beam G2 e = 30 mm

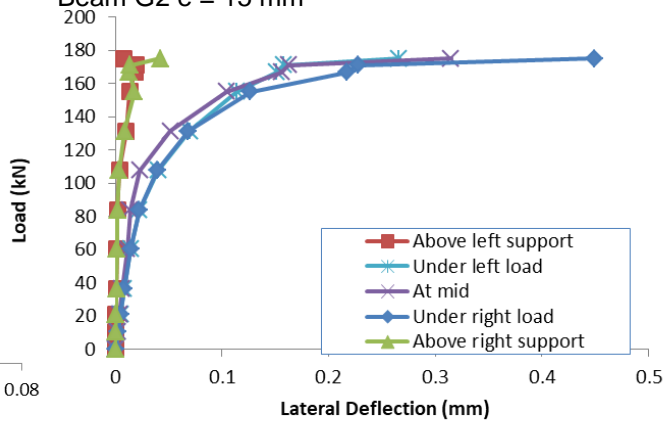


**Fig.8.** Typical Load-Lateral deflection curve of the Beam G2 e = 50 mm

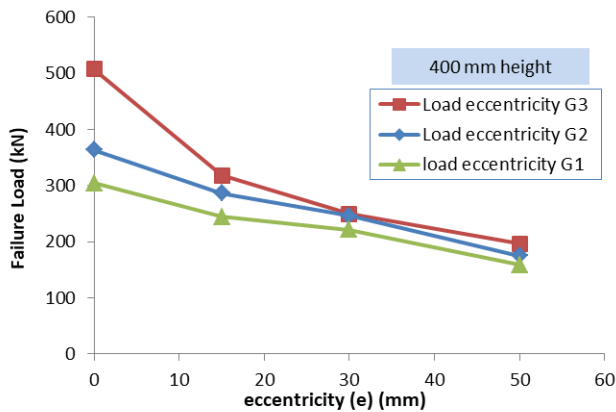


**Fig.9.** Dropping in Failure load due to applying load at e = (0,15, 30 and 50) mm

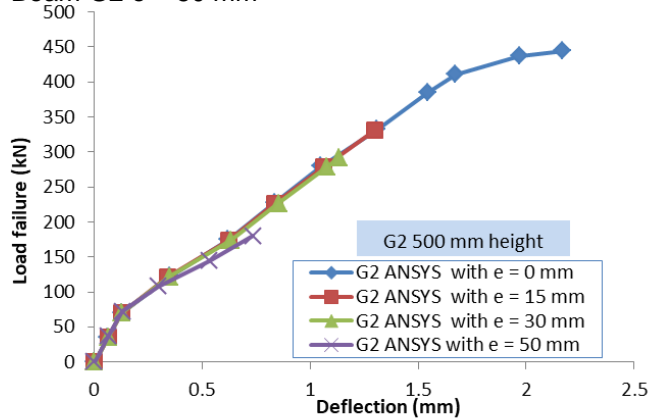


**Fig.10.** Eccentric Load-Deflection response of the Beam G2

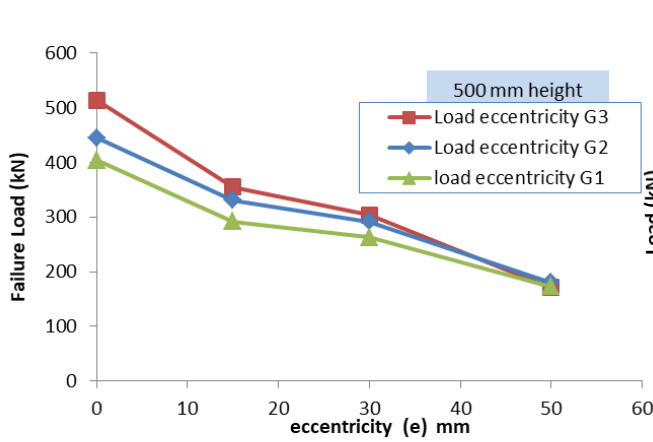


**Fig.11.** Dropping in Failure load due to applying load at  $e = (0, 15, 30$  and  $50)$  mm

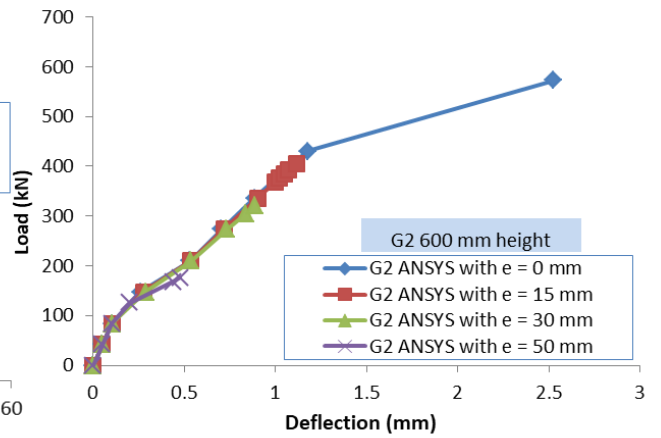


**Fig.12.** Eccentric Load-Deflection response of the Beam G2

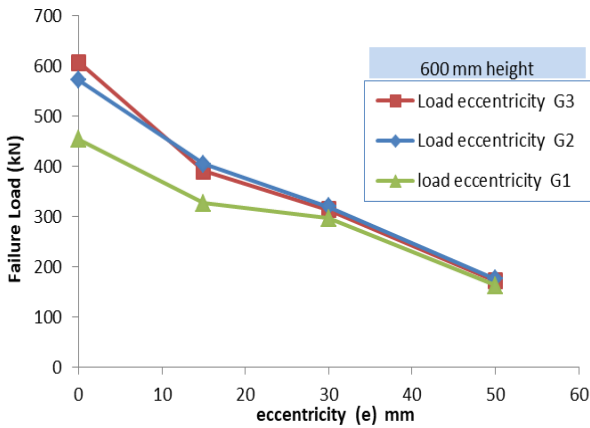


**Fig.13.** Dropping in Failure load due to applying load at  $e = (0, 15, 30$  and  $50)$  mm

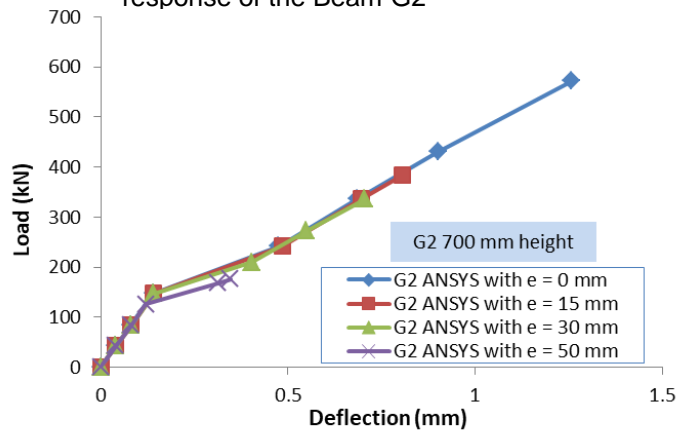


**Fig.14.** Eccentric Load-Deflection curve of the Beam G2

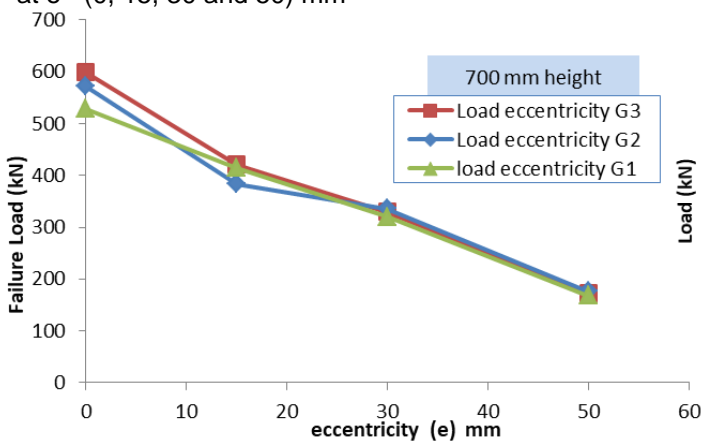


**Fig.15.** Dropping in Failure load due to applying load at  $e = (0, 15, 30$  and  $50)$  mm

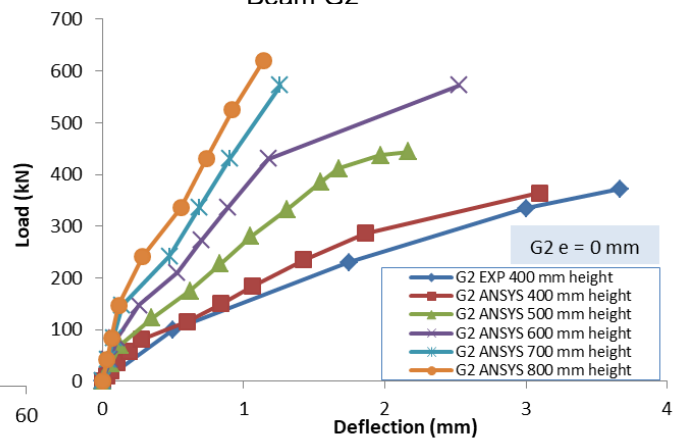


**Fig.16.** Load-Deflection response of the Beam G2

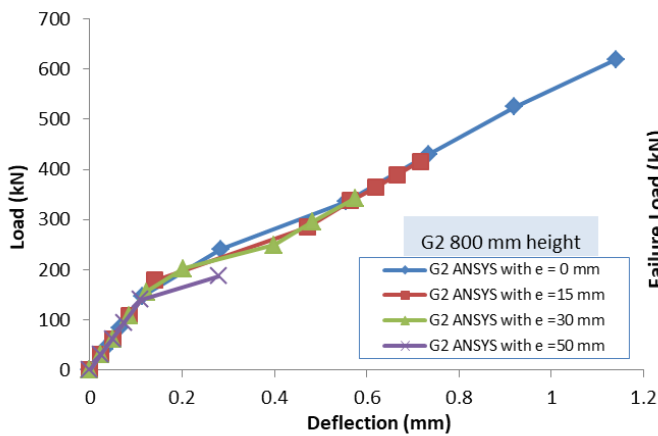


**Fig.17.** Eccentric Load-Deflection response of the Beam G2

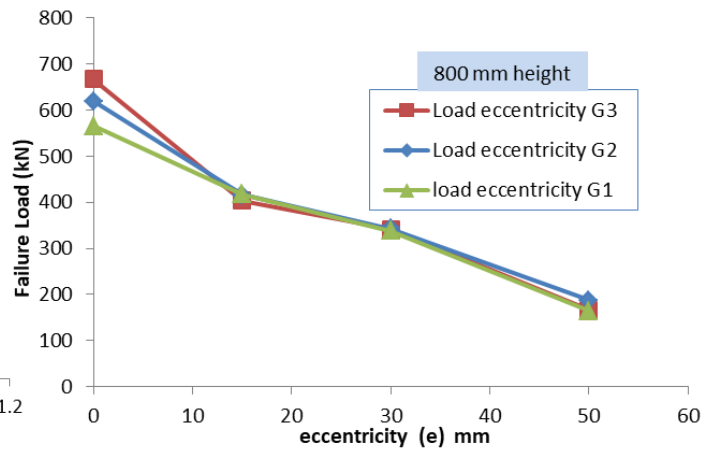


**Fig.18.** Dropping in Failure load due to applying load at  $e = (0, 15, 30$  and  $50)$  mm

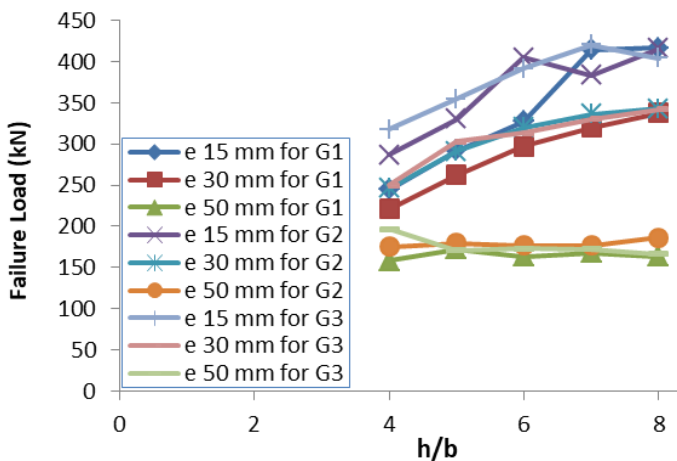


**Fig.19.** Change in the failure load of the beams G1, G2, G3 under eccentricity (0, 15, 30, 50) mm

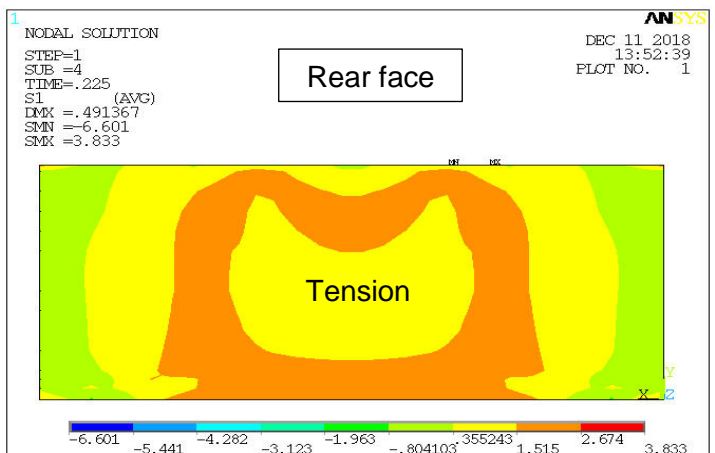
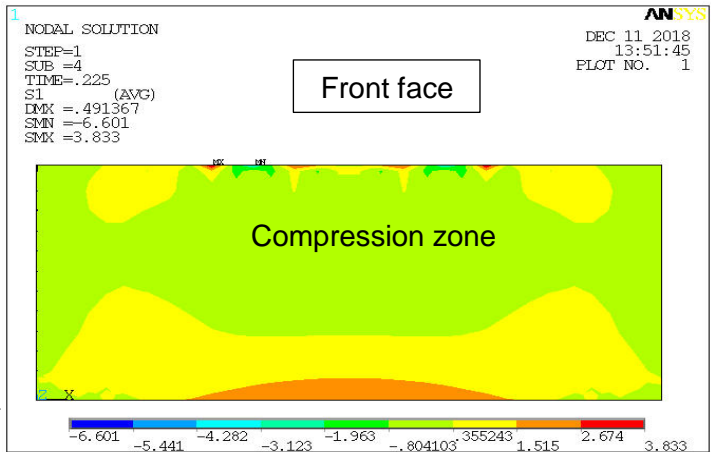


**Fig.20.** Typical principle stress S1 in beam G2. 800 mm height at 140 kN

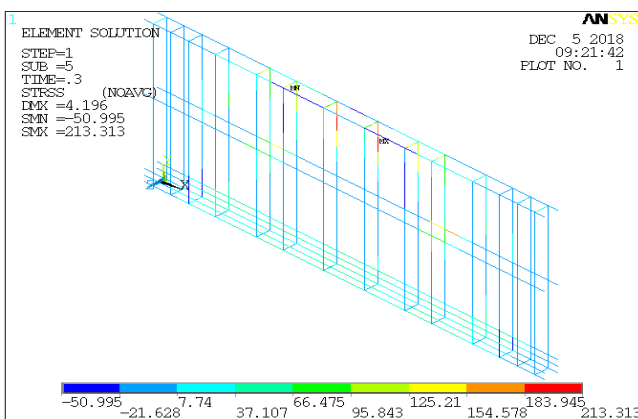


**Fig.21.** Typical stress in steel reinforcement S1 in beam G2, 800 mm height at failure

## 5. Conclusions

According to the present outcomes, it can be concluded that:

- 1- The general conclusion is that 3D ANSYS modeling is able to predict the load capacity failure for beams under eccentric load.
- 2- When the loads are applied perfectly concentrically, failure would happen due to shear, but when the loads are applied eccentrically, beams with eccentricity greater than 30 mm crushed at front the face of the beams at loads below their ultimate shear capacities.
- 3- The transition from shear to crush failure at the front face of the beams is often accompanied by a significant reduction in the ultimate load.
- 4- Eccentricity/thickness ( $e/b$ ) ratio is an important parameter in (out-of-plane) crushing.
- 5- The increases in the beams height lead to an increase in the failure load. But also a small eccentricity cause a clear drop in the failure load.
- 6- At  $e = 50$  mm, all beams with different heights have the same failure load.
- 7- When eccentricity increases the shear span has no effect on the failure load (increasing or decreasing).
- 8- The failure mode of the beams is concrete crushing, the compressive strength is the ruling control.
- 9- Deep beams offer an additional problem of excessive eccentric load which could result in a premature crushing collapse.

## REFERENCES

- [1] Yang KH, Ashour AF. Influence of section depth on the structural behaviour of reinforced concrete continuous deep beams. *Magazine of Concrete Research* 2007; **59** (8): 575–586.
- [2] Hanna ThH. Experimental Investigation of Static Behavior of Fibrous Concrete Simply Supported Deep Beams under Patch Loading. *Tikrit Journal of Engineering Sciences* 2012; **19** (3): 68-78
- [3] American Concrete Institute ACI 318M-14 Building Code Requirement for Structural Concrete. American Concrete Institute, USA. 2014
- [4] Tan KH, Kong FK, Teng S, Guan L. High-Strength Concrete Deep Beams with Effective Span and Shear Span Variations. *ACI Structural Journal* 1995; **92** (4): 395-405.
- [5] Siao WB. Shear Strength of Short Reinforced Concrete Walls, Corbels, and Deep Beams. *ACI Structural Journal* 1994; **91** (2): 123-132.
- [6] Patil SS, Shaikh AN, Niranjana BR. Non Linear Finite Element Method of Analysis of Reinforced Concrete Deep Beam. *International Journal of Modern Engineering Research* 2012; **2** (6): 4622-4628.
- [7] Plasencia GR, Rocha JDB, Santana JJH, Pudipedi L. Study of the behavior of reinforced concrete deep beams. Estimate of the ultimate shear capacity. *Revista de la Construcción* 2017; **16** (1).
- [8] Salamy MR, Kobayashi H, Unjoh Sh. Experimental and Analytical Study on RC Deep Beams. *Asian Journal of Civil Engineering (Building and Housing)* 2005; **6** (5): 487-499.
- [9] Lafta YJ, Kun Ye. Structural Behavior of Deep Reinforced Concrete Beams Under Indirect Loading Condition. *International Journal of Civil Aug* 2015; **5** (4): 53-72.
- [10] Sabale VD, Borgave MD, Joshi PK. Non-Linear Finite Element Analysis of Deep Beam. *International Journal of Engineering Research & Technology* May 2014; **3** (5): 2135- 2139
- [11] Kumar KK, Ramadass S. A Study on Concrete Deep Beams using Nonlinear Analysis. *International Journal for Innovative Research in Science & Technology* October 2015; **2** (5): 57-64.
- [12] Chemrouk M. Slender Concrete Deep Beams: Behaviour, Serviceability And Strength. Ph.D. thesis. Newcastle University; Upon Tyne; England: 1988.
- [13] Belhacene A, Bouhaloufa A, Zelat K, Kadri T, Bekouche MS. High Strength Eccentrically Loaded Slender Reinforced Concrete Deep Beams with Vertical Edge Restraint. Conference on the bridge behavior 2016 20 June; Istanbul, Turkey
- [14] Kim HS, Lee MS, Shin YS. Structural Behaviors of Deep RC Beams under Combined Axial and Bending Force. *Procedia Engineering* 2011; **14**: 2212–2218
- [15] CIRIA GUIDE 2. the Design of Deep Beam In Reinforce Concrete. Construction industry research and information association. Westminster, London. (1977).
- [16] Euro code 2. Design of concrete structures-part 1: General Rules and Regulations for buildings. English Edition, British Standards Institution, London, 1992.
- [17] Portland Cement Association. Tilt-up Load-bearing Walls – A Design Aid. Publication No.EB074.02D, Illinois, 27pp. 1979.
- [18] ANSYS, Inc., "ANSYS Help", Release 11.0, Documentation, Copyright 2007.
- [19] Willam KJ, Warnke EP. Constitutive Model for the Triaxial Behavior of concrete. International Association for Bridge and Structural Engineering 1975; **19**: 174.
- [20] Desayi p, Krishnan s. Equation for the Stress-Strain Curve of Concrete. *Journal of the American concrete Institute* 1964; **61**: 345-350.
- [21] Ismail KS. Shear Behaviour of Reinforced Concrete Deep Beams. Ph.D. thesis. Sheffield University; Sheffield; England: 2016